Scale Decompostion In Burgers' Equation

Frédéric Heurtaux* Fabrice Planchon†
Mladen Victor Wickerhauser‡

Department of Mathematics, Campus Box 1146
Washington University in St. Louis, MO 63130

June 6, 1993

Abstract

The wavelet representation of a time-dependent signal can be used to study the propagation of energy between the different scales in the signal. Burgers' evolution operator (in 1 and 2 dimensions) can itself be described from this scaling point of view. Using wavelet-based algorithms we can depict the transfer of energy between scales. We can write the instantaneous evolution operator in the wavelet basis; then large off-diagonal terms will correspond to energy transfers between different scales. We can project the solution onto each fixed-scale wavelet subspace and compute the energy; then the rate of change of this energy by scale can detect and quantify any cascades that may be present. These methods improve the classical Fourier-transform-based scale decomposition which uses the notion that wavenumber equals scale. The wavelet basis functions underlying our scale decompositions have finite, well-defined position uncertainty (i.e., scale)

*Supported in part by the Internship Office of the Ecole Polytechnique.
†Supported in part by the Internship Office of the Ecole Polytechnique.
‡Supported in part by the Air Force Office of Scientific Research.

whereas Fourier basis functions have formally unbounded position uncertainty.

1 Introduction

The difficult problem of turbulence in fluids has spawned a rich variety of ideas and notions of measurement. A fluid flow contains a very large number of degrees of freedom, and yet there are certain identifiable features which can be described at least approximately with a small number of parameters. For example, in viscous fluids the large regions of high vorticity seem to evolve in a coherent manner. The number of such regions is necessarily limited and their sizes and shapes change quite slowly. These have been quite successfully modelled by point vortices and particle mechanics [3], point vortices with a few extra moments [2], and contour dynamics [15], all of which techniques replace the grid point approximation by a much lower rank approximation and rewrite the equations of motion in terms of the new parameters. It is also possible to compute various averages and show from first principles that they are conserved, or change monotonically, or have specified behavior when a particular term of the differential equation is dominant. Such quantities include total energy, total enstrophy and average velocity, which can be calculated using Newton's laws of motion or other conservation principles.

The famous 1941 paper by Kolmogorov [10] predicted that the energy spectrum of the velocity field of fully developed turbulence should be modelled by a $k^{-5/3}$ power law (in the wavenumber k). One intuitively compelling explanation for this relationship is that energy flows from large-scale coherent velocity fields to small-scale dissipative eddies. However, it has been difficult to quantify this notion, partly because it is difficult to define scale in a satisfactory manner. Traditionally, scale has been set equal to wavenumber k in the Fourier transform of the velocity field. The energy at a given scale was then defined to be the sum of the squares of the Fourier coefficients in a certain range of wavenumbers. Unfortunately, the operation of restriction to a range of wavenumbers is ill conditioned in any norm but L^2, it is equivalent to projection onto basis functions which have no well-defined scale, and can mislead the aforementioned intuition simply by its mathematical ill-behavior. Our goal in this paper is to replace the Fourier–wavenumber "scale" projection with a mathematically better-behaved alternative of wavelets. We can

then exploit this new wavelet scale projection to measure energy transfers between scales in a particular solution to Burgers' equation, a simplified fluid flow equation [5].

For turbulent flows, Kolmogorov, Kraichnan [11] and Batchelor [?] predicted that the energy repartition depends on the scale of the structures that appear in the flow. Wavelets are an especially suitable tool for problems involving scale, since every wavelet has a well-defined scale of its own. We can define the *energy of a function at a scale* σ simply by summing the squares of the amplitudes of all wavelets of scale σ in the function. We can then ask how energy is transferred between scales in an evolving turbulent flow. To approach this question, we will consider Burgers' equation in one dimension, where exact analytic expressions of the solution are known for some initial condition. We will first see how the small scale wavelets in the decomposition of the solution collect more and more energy as the evolution proceeds and approaches singularity. We will also describe the time-varying Burgers evolution operator corresponding to a known evolution. We will conjugate it into a matrix with respect to the wavelet basis, where scales can be easily identified. We will observe those matrix coefficients which couple the different scales and transfer energy between them. We can thus observe the creation and destruction of small-scale phenomena such as rapid fluctuations or "shocks." We will also repeat a part of this analysis for the two-dimensional Burgers equation, to see if our surmises hold in that more complicated situation.

In related work [7], an intial parameter reduction by projection onto just the largest wavelet packet coefficients was compared to parameter reduction by projection onto low wavenumbers. This provides another test of the notion that energy cascades from large wavelengths to small. The main purpose of that paper, however, was to test how well the reduced-parameter flow predicts the original, reference flow; it demonstrated that projection onto large wavelet packets is substantially better than projection onto low wavenumbers, in both a deterministic and statistical sense. In other related work [12] an adaptive algorithm used wavelets to perform the numerical integration of Burgers' equation. When the energy in some range of small scales exceeds a threshold in a region, then the solution is resampled more finely in that region. While the methods discussed in this present paper are intended only to suggest how to quantify certain intuitive notions, they are oriented toward improving the numerical solution of fluid dynamics problems by similar

adapted algorithms.

2 Burgers' evolution equation

Burgers' equation is the first part of the following initial value problem:

$$\frac{\partial F}{\partial t}(x,t) = -\frac{1}{2}\frac{\partial}{\partial x}F^2(x,t) + \nu\Delta F(x,t); \qquad F(x,0) = F_0(x). \tag{1}$$

The constant ν is the viscosity of the fluid and the function $F_0 = F_0(x)$ is the initial state at time $t = 0$.

Let us consider one example: $F_0(x) = \sin(2\pi x)$. The graph in Figure 1 shows the evolution of this function at times 0, 0.08, 0.16, 0.32, 0.5, 0.75, and 1.00. The two arcs of the sine, one positive the other negative, are propagating in opposite directions to produce a steep slope at $x = 32/64$. The dissipative term ΔF produces the vanishing effect: the total energy in the solution tends to 0 as time increases. Without dissipation the slope at $x = 32/64$ would become infinite and a discontinuity would appear; the viscosity term controls how close the solution gets to singularity before dissipating. The apparition of a near-discontinuity means that the amplitudes of small-scale wavelets in the solution are increasing, since they contribute the large derivatives. We can effectively see this phenomenon in Figures 2 and Figure 3. The graduations between 0 and 100 represent time; the others show the index of the wavelet coefficients. The first wavelet coefficient is the mean of the signal (actually 0), the second is the biggest-scale difference coefficient, and so on. The last 32 are the smallest scale difference coefficients, since we took 64 samples of the signal. We use the "Coiflet" wavelets based on a quadrature mirror filter with 30 taps [6] because they have a large number of vanishing moments and are nearly symmetric.

We computed the evolution with a Godounov scheme applied to the 1-periodic signal, using a space-step of 1/64 and a time step of 1/100. Figures 2 and 3 show the evolution of wavelet coefficients. They indicate that the energy in the biggest-scale wavelets is decreasing while the energy in the smallest-scale ones is increasing. In the view from below (Figure 3), we observe that one of the big-scale amplitudes already begins to decrease at time zero. Figure 2 shows that the maxima of the smaller-scale amplitudes are reached later and later with decreasing scale. This last aspect can be better

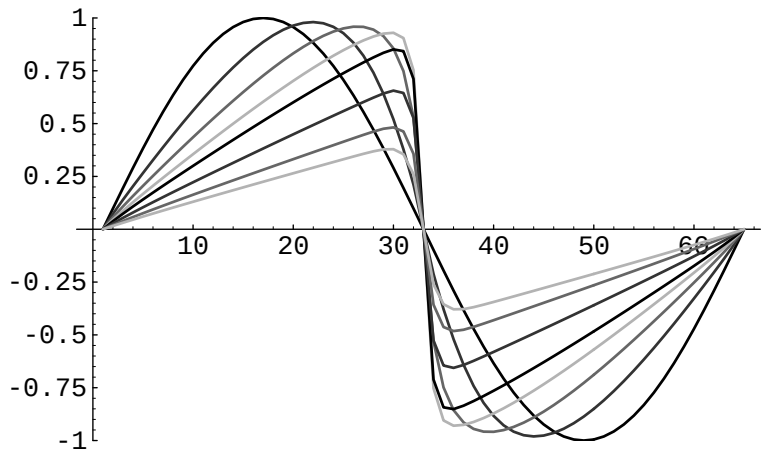

Figure 1: Evolution of $\sin(2\pi x)$ over [0;1].

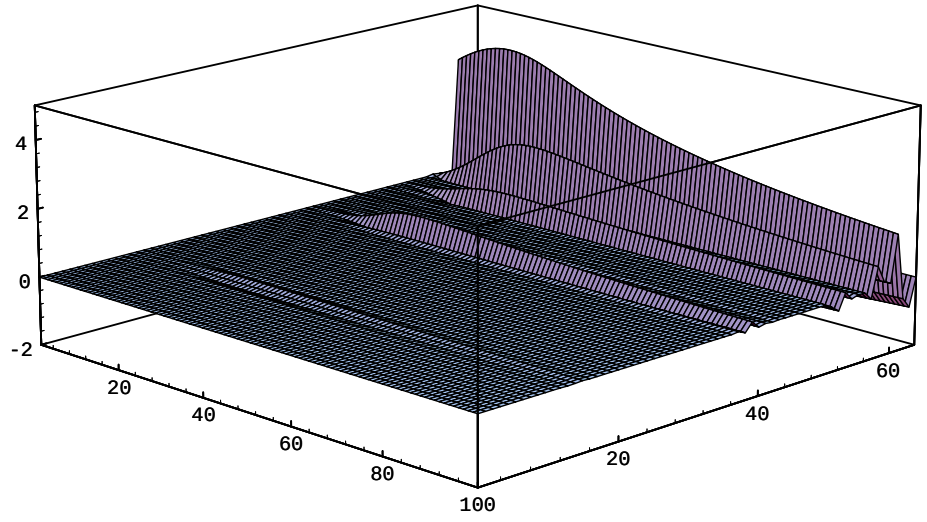

Figure 2: Evolution of the wavelet coefficients.

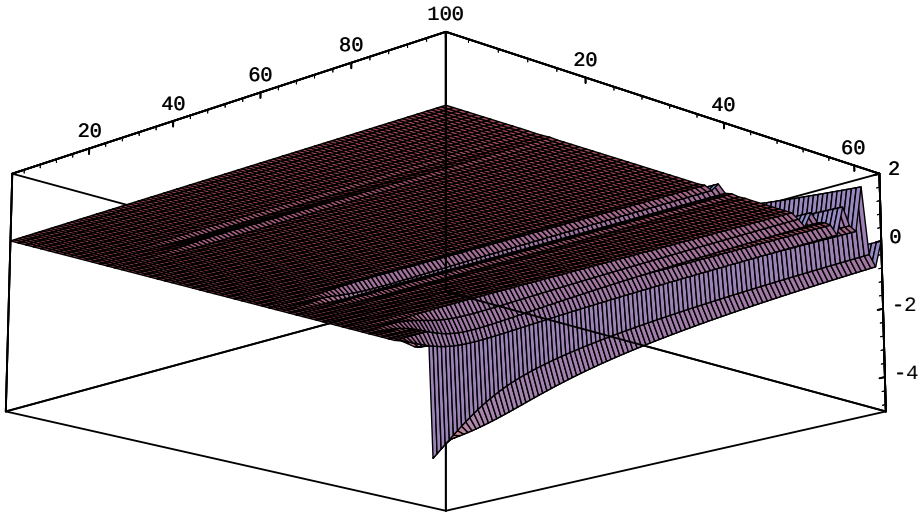

Figure 3: Same 3D representation, seen from below

seen on Figure 4 which shows the absolute value of the wavelet coefficients in gray scale: white is zero, black is the maximum.

Ultimately, all the wavelet coefficients decrease to 0, because through dissipation the energy in the signal decreases to 0.

3 Burgers' evolution operator

We will now try to extract inter-scale energy transfer information from the evolution operator of Burgers' equation. In fact, we will use the infinitesimal generator of the evolution, which is the Jacobian of the right-hand side of Equation 1.

Let G be the matrix of our transformation using the Godounov scheme in the normal space, and W be the matrix of our wavelet transform. Let $u(x,t)$ (or simply $u(t)$ but actually $u(i\Delta x, n\Delta t)$) be our signal, and $U(t)$ be its wavelet form. We have:

$$u(t+\Delta t) = Gu(t); \qquad U(t+\Delta t) = (WGW^{-1})U(t) \tag{2}$$

Figure 5 shows the coefficients of $K = WGW^{-1}$ at times $t = 0.00$ on the left and $t = 0.33$ on the right. In the density plots, black means the

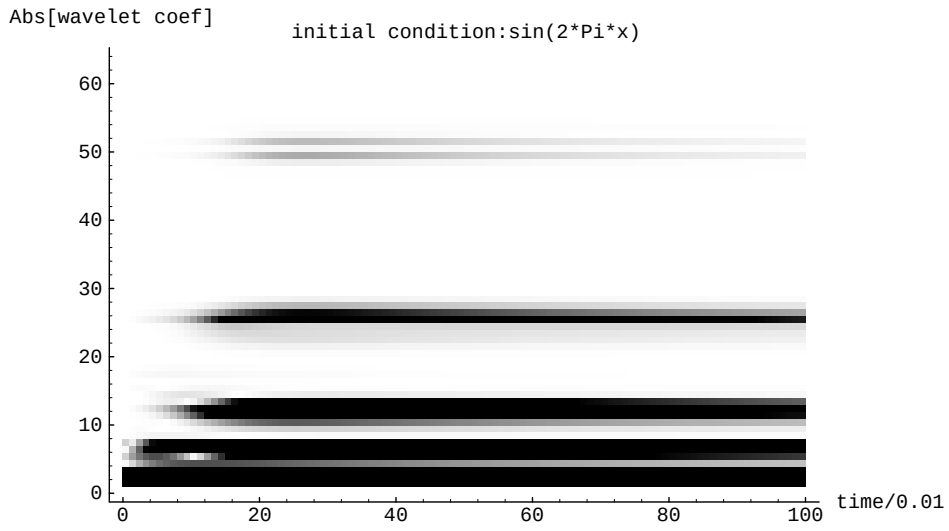

Figure 4: Time evolution of the wavelet coefficients in gray scale

minimum and white means the maximum, with gray being zero. We are using the classical form of simple operators in the wavelet basis, the so-called "standard form" of G. Beylkin, R. Coifman and V. Rokhlin (see [4]). The "fingers" which lay across the matrix density plots represent strong coupling between wavelet scales. The main diagonal is the coupling between wavelets at equal scales, the upper triangle fingers are couplings from large scales to small scales, and the lower triangle fingers are couplings from small scales to large scales.

The isolated dark points in the last row and last column of each matrix are not artifacts of the periodization, but are due to the periodicity of each block itself in the matrix, and also to the discontinuity introduced by the Godounov scheme in the derivative at this point.

Unfortunately, it is not easy to read Figure 5. We see in the right-hand picture that the scale interactions mainly occur in the high-gradient zone of the signal near the "midpoint," where the large amplitudes in K show up as fingers. We can observe that the strongest interactions take place between nearby scales, since the variation from gray is strongest along the middle fingers and decreases away from the main diagonal. We can also say that

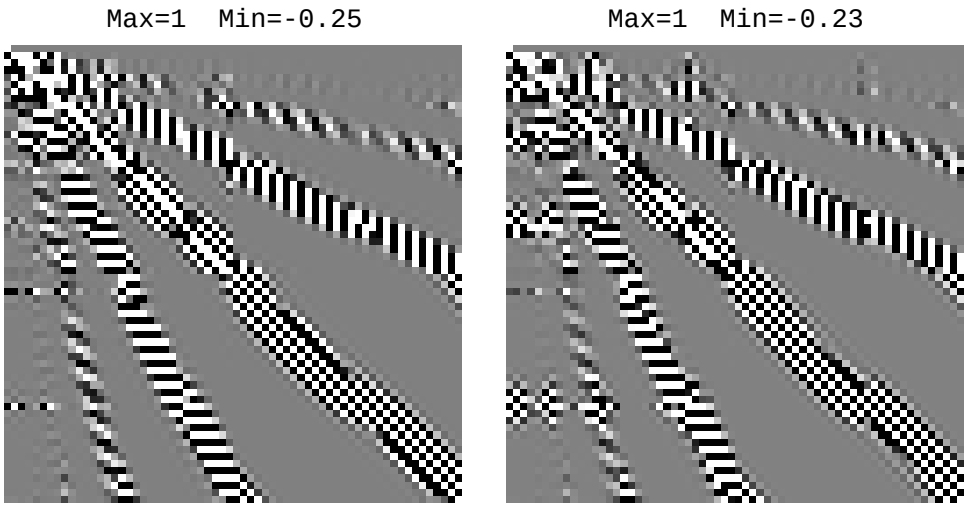

Figure 5: Burgers' evolution operating on wavelet components

the interactions between the largest and smallest scales become stronger as the solution evolves, since the outside fingers become thicker as t increases. But it is impossible to say what kind of interactions these are, since the coefficients are alternately positive and negative.

To see where the energy is concentrated, we now study the effects of Burgers' evolution operator on the absolute value of the wavelet coefficients in our signal. The sums of these absolute values is what we shall call "energy." Let $|U|$ denote the absolute value of these coefficients, let S be the diagonal "sign matrix" made of the signs of these coefficients, and let I be the identity matrix. We have:

$$\begin{aligned}
\frac{\partial |U|(t)}{\partial t} &\approx \frac{|U|(t+\Delta t) - |U|(t)}{\Delta t} && (3)\\
&= \frac{1}{\Delta t}(|WGu| - |Wu|)(t) && (4)\\
&= \frac{1}{\Delta t}(|WGW^{-1}Wu| - SWu)(t) && (5)\\
&= \frac{1}{\Delta t}(|WGW^{-1}SSWu| - SWu)(t) && (6)\\
&\approx \frac{1}{\Delta t}(SWGW^{-1}S - I)|U|(t) && (7)
\end{aligned}$$

The last approximation assumes that $WU(t + \Delta t)$ and $WU(t)$ have the same sign matrix. Since the wavelet coefficients are continuous, slowly varying functions of time, this assumption will only be violated by coefficients close to 0 whose error contribution is therefore small. The new matrix $R = SWGW^{-1}S - I$ is not really simple to understand either, even if we only keep the sign of its most significant coefficients, the ones greater than 0.5% of the maximum coefficient, as in the right picture of Figure 6. The matrices shown in that figure have the following block structure:

-1/-1	0/-1	1/-1	2/-1	$\cdots$	5/-1
-1/0	0/0	1/0	$\cdots$	$\cdots$	5/0
-1/1	0/1	1/1	$\cdots$	$\cdots$	5/1
.	.	$\cdots$	$\cdots$	$\ddots$	$\cdots$
-1/5	0/5	1/5	2/5	$\cdots$	5/5

Each block i/j represents the part of the matrix corresponding to the influence of scale i on what the scale j will be at the next time step. Scale -1 is the mean of the signal, a single value. Scale 5 is the smallest scale and contains 32 components.

In order to get more readable results, we now forget about the space localization of the signal and only look at how the different scales act upon

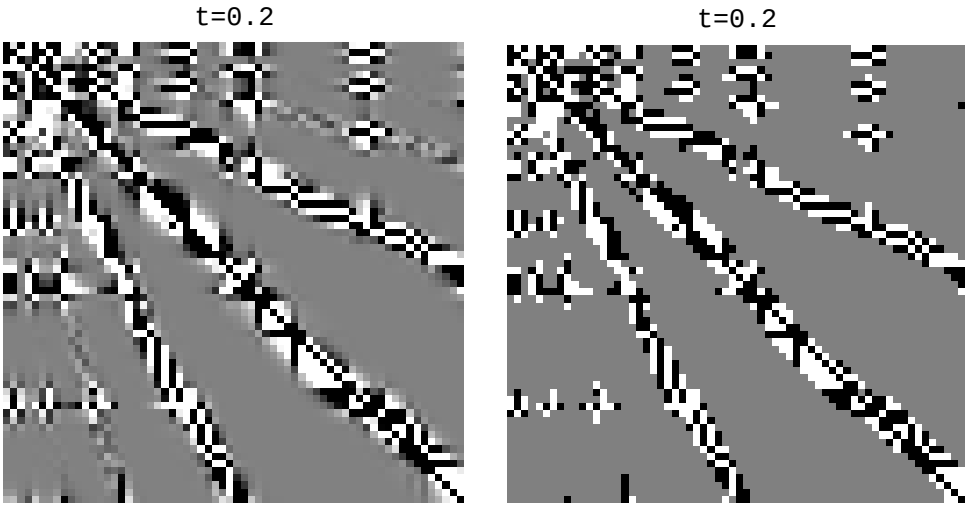

Figure 6: Evolution matrix of $|U|$

each other. We sum the amplitudes of each block of the evolution operator to one characteristic value, the contribution of all wavelets at one scale i to the sum of the absolute values of the wavelet coefficients for another scale j. To do this we first set to zero all coefficients of the evolution matrix outside the block (i/j), then multiply it by $|U|$ and sum all the coefficients of the result. We thereby obtain a "matrix of energy transfers between scales." It displays the expected phenomenon: the energy of the biggest scales flows to the smallest ones. Figure 7 shows an example of this matrix at one particular time. It is possible to compute this matrix at each time step and to prepare an animation of the result; this has been done, and the data is available by anonymous ftp [9].

The contributions of the different scales can determined fom the sign of the histogram in Figure 7. The coefficients above the diagonal are negative, while those below the diagonal are positive. The negative superdiagonal elements show that the small scale components draw energy from larger scales. Likewise, the positive subdiagonal coefficients indicate that big scale components contribute energy to the creation of small scale components. The structure of this energy transfer matrix changes rapidly between $t = 0.00$ and $t = 0.15$, and then remains stable in the form shown above.

If we now want to know how the energy concentrates itself in certain

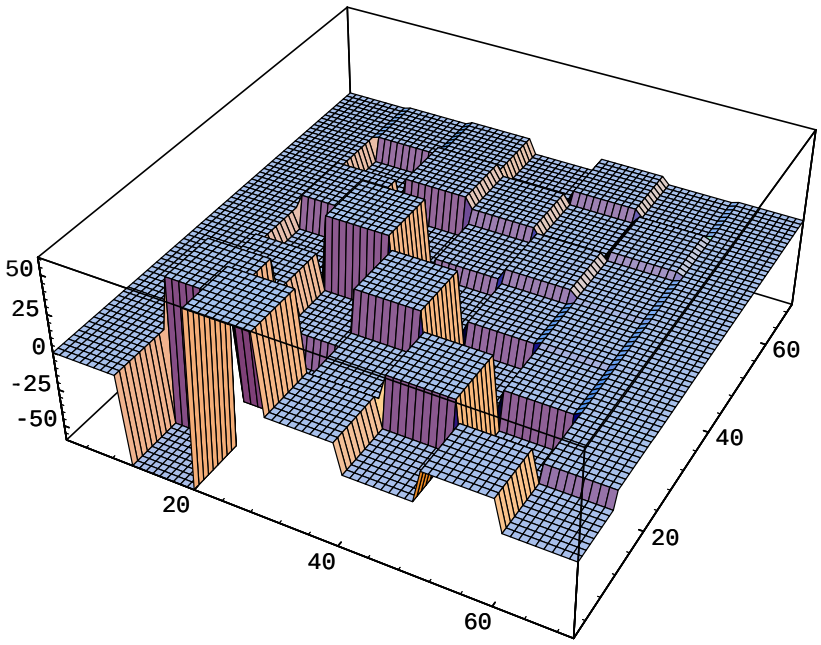

Figure 7: Matrix of interactions between scales at time equals 0.2

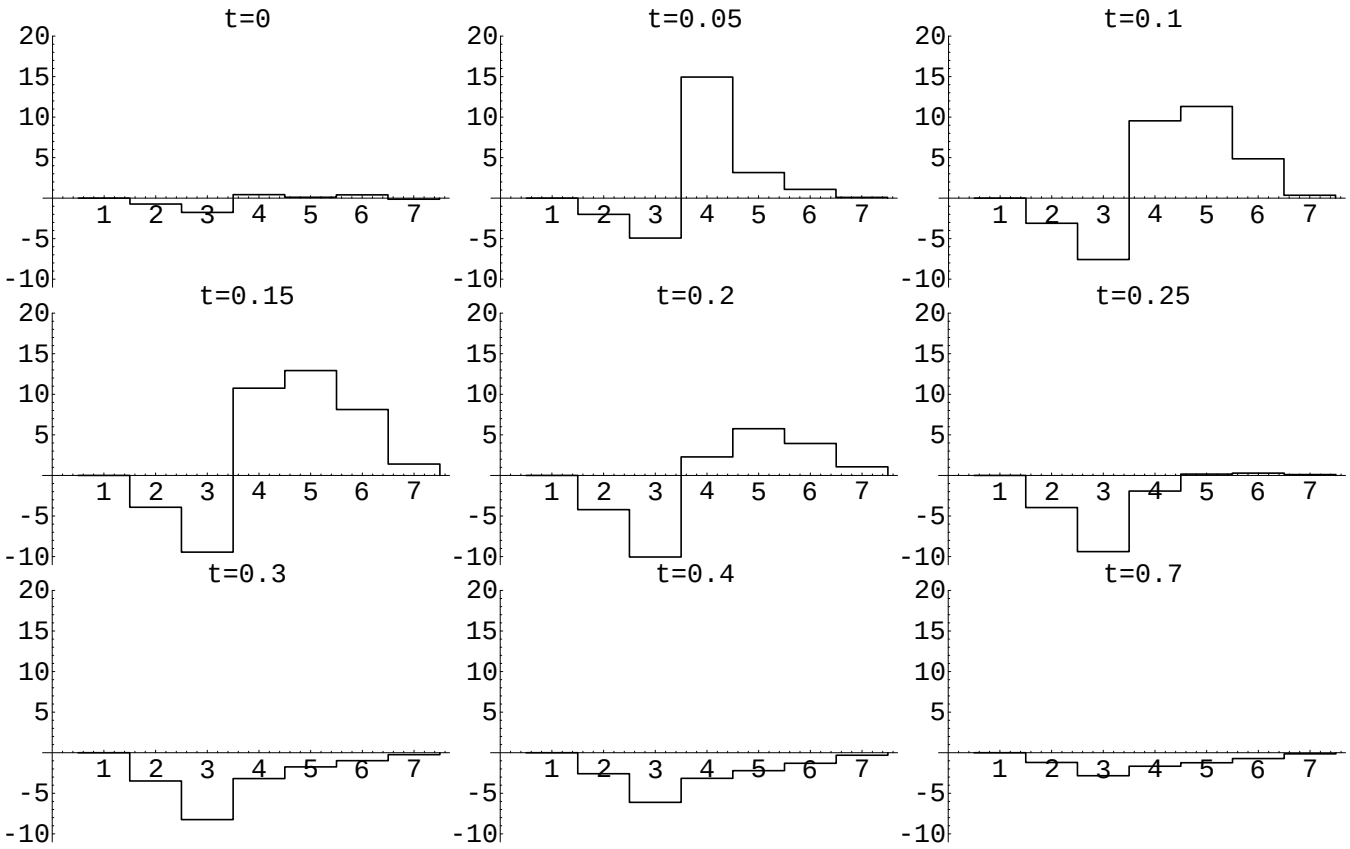

Figure 8: Time derivative of the "energy" contained in each scale

scales, we only have to multiply this matrix by the vector $(1, 1, \ldots, 1, 1)$ to sum over all contributions. We then obtain the results in Figure 8. From this collection of snapshots, taken at different times, we can see the derivative evolution of the sum of the absolute values of the wavelet coefficients for each scale: the scale whose energy increases fastest changes with time, from scale 3 (where there are 4 coefficients) at time $t = 0.00$ to scale 5 (where there are 16 coefficients) at time $t = 0.70$. Note that the scale graduations are shifted by one. The energy comes from the biggest scales, where it always decreases. The last three pictures show the final phase of the evolution, when the signal collapses. All appears as if Burgers' evolution operator is propagating the energy down through the scales from the biggest ones to the smallest ones.

4 Other examples

We now study a less particular example, one in which there is propagation of the region where the small scales develop. This example is obtained simply by subtracting the constant $\frac{1}{\sqrt{2}}$ from our sine function.

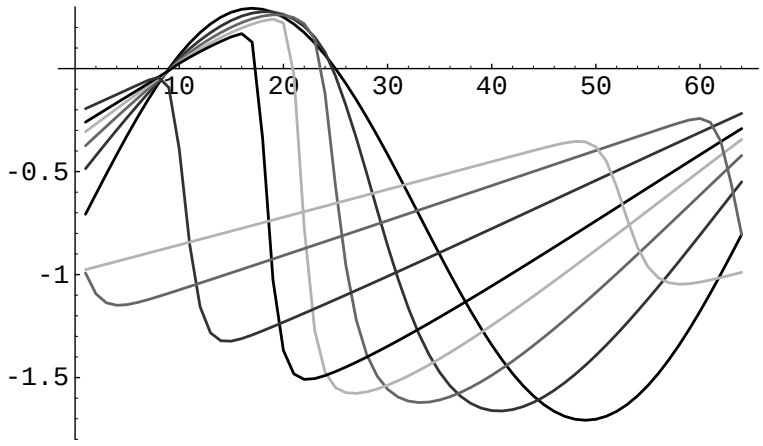

Figure 9: Evolution of $\sin(2\pi x) - 0.707$, $x \in [0, 1]$.

Figure 9 shows the propagation we get with this signal. The graphs show the signal at times 0.00, 0.08, 0.16, 0.24, 0.32, 0.50, 0.75 and 0.99. The two inflection points of the signal translate with a slowly varying speed which we

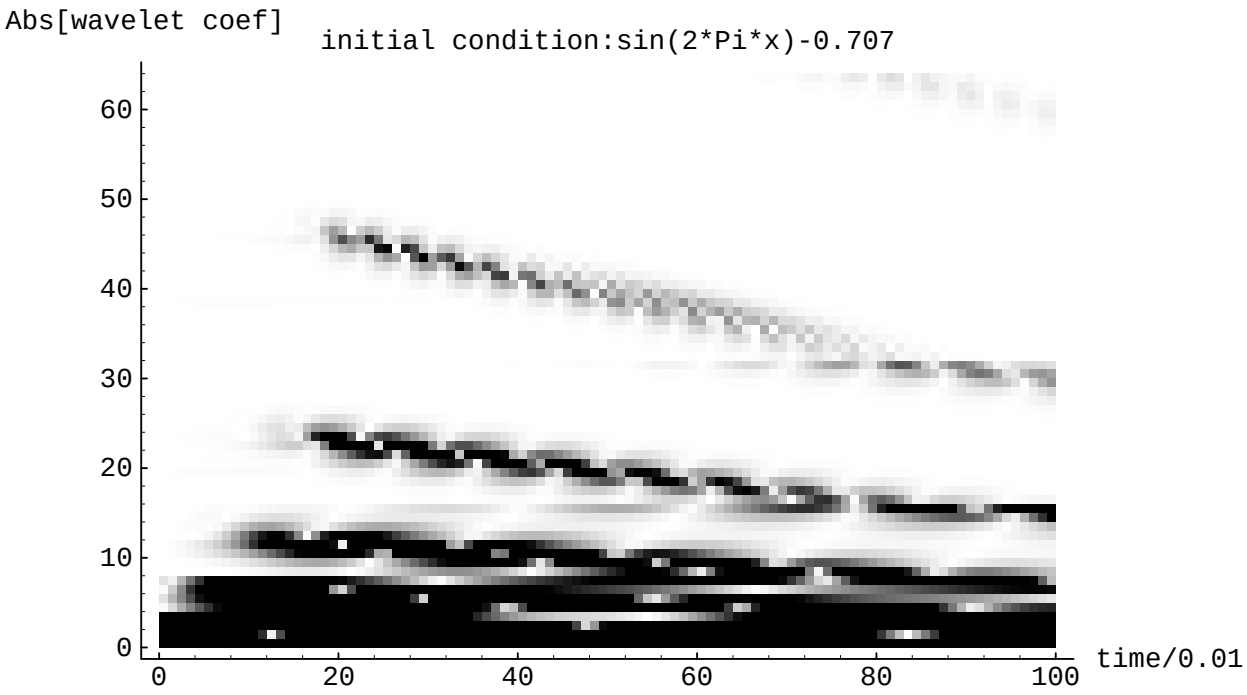

Figure 10: Time evolution of the absolute value of the wavelet coefficients in the previous figure, in gray scale

may call the *speed of propagation*. Because of this propagation, we observe dyadic artifacts due to the relative motion between the signal and the wavelet centers. For instance, when the function $\sin(2\pi x)$ is translated along the x-axis by amounts which are less than the nominal support of the smallest wavelet, its periodic wavelet transform on $[0,1]$ changes rather dramatically with each translation step. Such translation produces not only phase shifts in the wavelet coefficients, as is the case with Fourier coefficients, but also rather complicated amplitude variations. The amplitudes at each wavelet scale oscillate several times with a mean period roughly equal to the scale length divided by the propagation speed.

Figure 10 shows the evolution of the wavelet coefficients of the signal in Figure 9 in gray scale. Notice that the large amplitude, small-scale wavelets cluster around the signal's region of largest derivatives, which propagates. Note too that the smaller-scale wavelets develop significant amplitudes later and later in the evolution. Compare this picture with Figure 4 and observe that the lack of symmetry in the solution does not interfere with the appearance of small-scale wavelets.

The spatial localization of wavelets is used only to define a mathematically acceptable notion of scale. Since we are interested only in the scale of the energetic components, and not in their spatial location, we can average over all shifts the absolute value of the wavelet amplitudes at a given scale to get a shift-invariant measure of energy in that scale. That is to say, we define the energy in a scale i to be the average over all translates by 1 of the sum of the absolute values of the amplitudes of all wavelets at scale i. We can compute these sums simply by making an average over all the possible shifts of the signal. In fact, it is possible to do this average over two shifts for the smallest scale, four shifts for the next bigger, and so on. We need all the shifts only for the biggest scale; the sum at scale s (with $s = 1$ being the smallest scale) is a 2^s periodic function of the shift. Such averaging will smooth out most but not all of the oscillations; there will still be some oscillations which are caused by translations on a scale smaller than that of the finest spacing of our dyadic grid. This unavoidable portion of the oscillation phenomenon can be seen on Figure 11, showing the same thing as Figure 8, but for the shifted sine propagation.

Oscillations make reading the energy difficult. We must determine the amplitude of the oscillations despite their irregularity, in order to do the same as what is shown in Figure 8. After averaging over shifts we obtain a mean

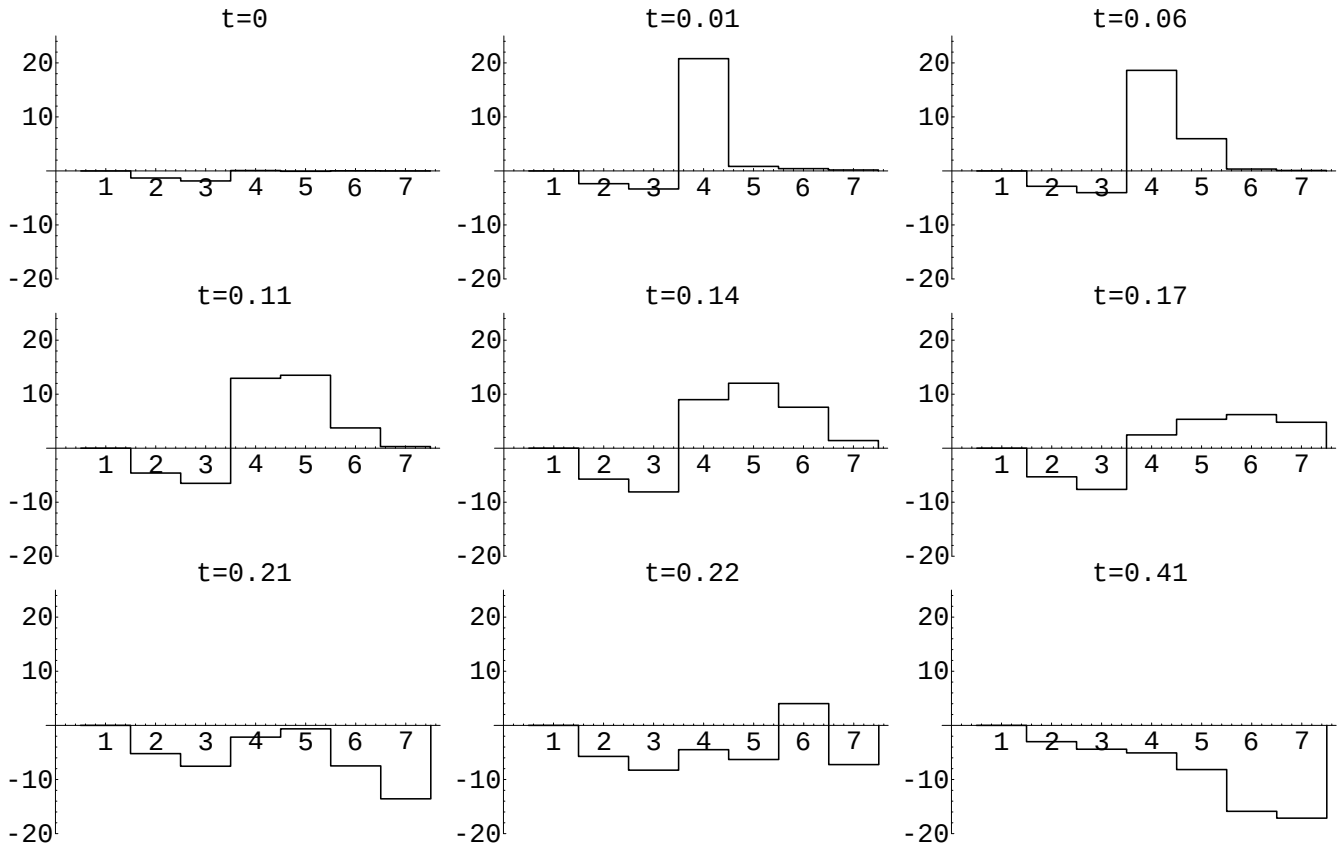

Figure 11: Time derivative of the "energy" contained in each scale, with averaging over shifts.

period for the remaining oscillations. The results of this averaging are shown in Figure 10. The six first pictures can be interpreted exactly the same way as for $\sin(2\pi x)$, but the three last show that this interpretation breaks down with time. For example, between $t = 0.20$ and $t = 0.21$ there is an important variation of the derivative of the energy located in each scale.

The interaction matrices in Figures 12–15 are quite interesting, too. They show that as soon as each scale develops enough energy, it positively affects the immediately finer scale. At the beginning, we can also see that some big scales transfer their energy to almost all finer scales. We can also see that after a certain time, the smallest scales contribute negatively to the greater scales.

Although the experiments are not included in this article, we remark that the same type of energy transfer occurs if we start with a Gaussian instead of a sine or a shifted sine function.

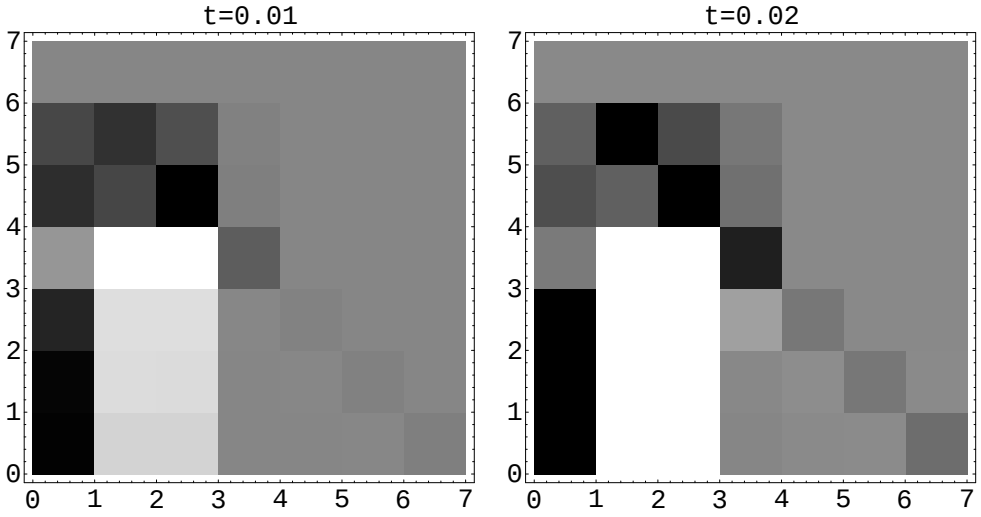

Figure 12: Matrix of interaction between scales: time steps 1, 2

5 Two Dimensions

We have also computed an analogous wavelet decomposition of the energy transfer phenomenon in the two dimensional case. We started with two

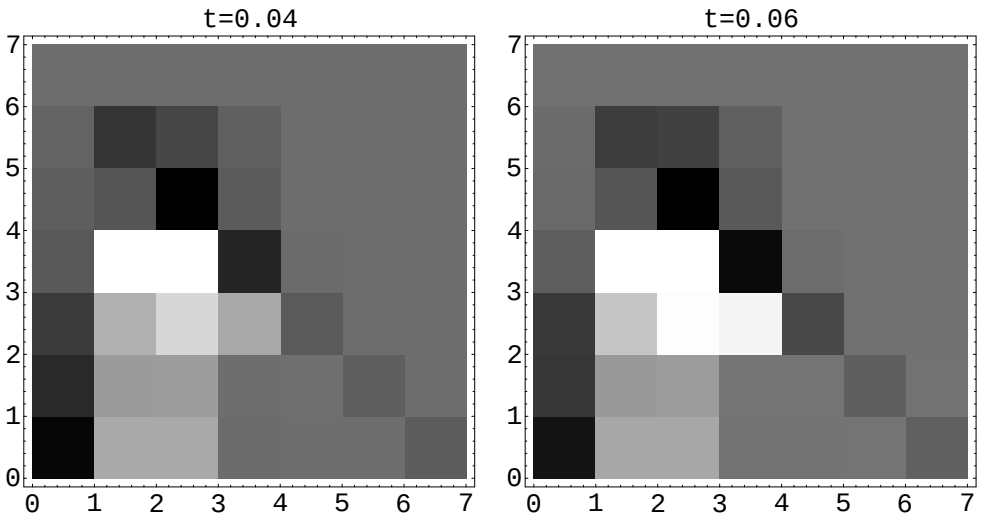

Figure 13: Matrix of interaction between scales: time steps 4, 6

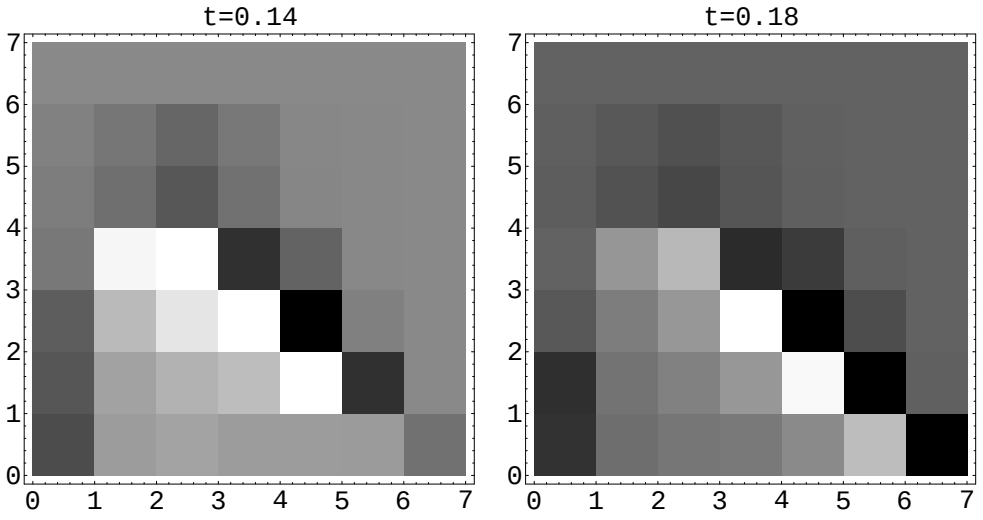

Figure 14: Matrix of interaction between scales: time steps 14, 18

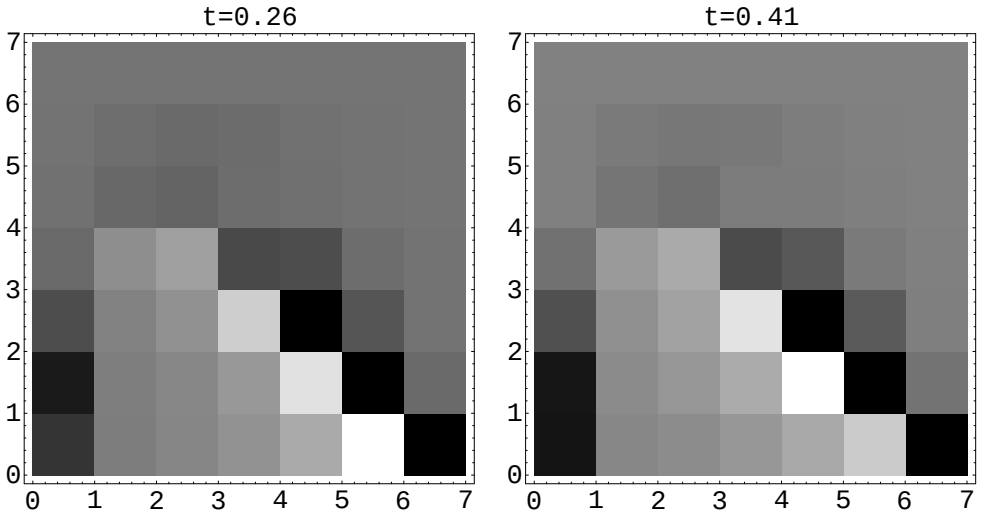

Figure 15: Matrix of interaction between scales: time steps 26, 41

bumps, one negative and the other positive, and crashed them into one another much as in the unidimensional case. The evolving signal, sampled on a 64×64 grid over 100 time steps, is displayed in the left-hand parts of Figures 16, 17, 18, and 19. The associated 4096×4096 instantaneous evolution operator is far too complicated to analyze in detail, so we limited ourselves to studying transfers of total energy among the 6 (isotropic) scales in that picture. This gave the much simpler 6×6 energy transfer matrix visible in the right-hand parts of Figures 16, 17, 18, and 19. The bidimensional signal exhibits similar variations of its summed absolute wavelet amplitudes as the unidimensional signal.

6 Future directions

These computations make rigorous the notion of energy transfer between scales within a solution of the 1-dimensional Burgers equation. To go further in this direction, we could refine the analysis to determine how energy is transferred between scales at each spatial location. This might introduce some additional dyadic grid artifacts, such as were already present in the propagating solution analysis. It is thus difficult to describe the instantaneous evolution operator at a fixed time step.

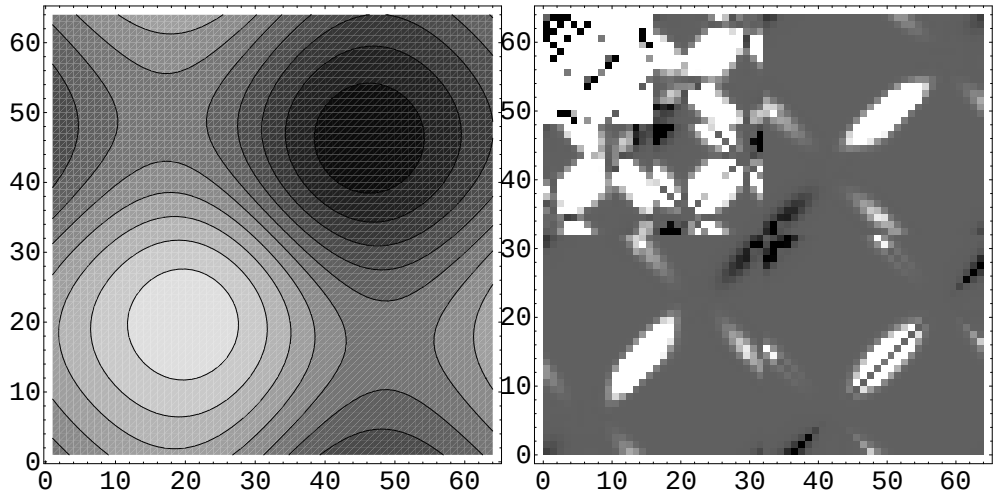

Figure 16: Signal and time derivative of wavelet coefficient absolute values at $t = 0.10$

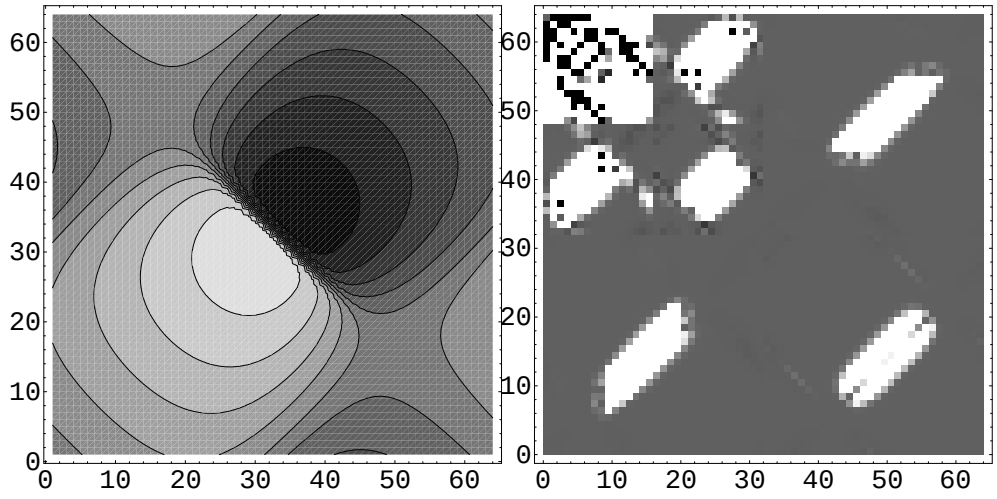

Figure 17: Signal and time derivative of wavelet coefficient absolute values at $t = 0.50$

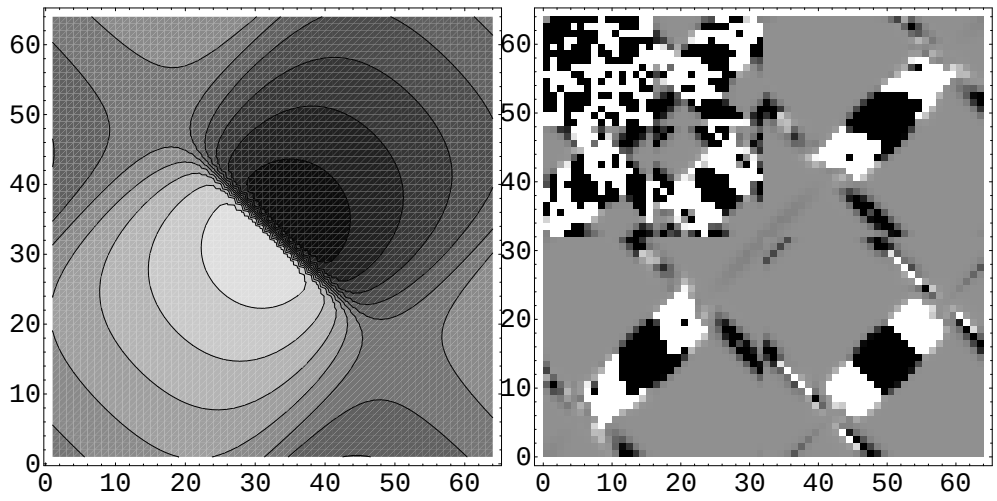

Figure 18: Signal and time derivative of wavelet coefficient absolute values at $t = 0.60$

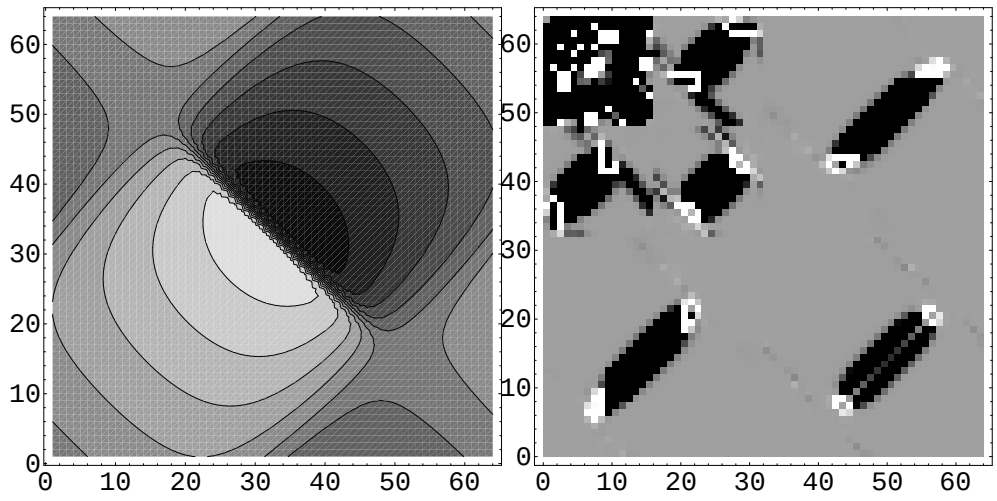

Figure 19: Signal and time derivative of wavelet coefficient absolute values at $t = 1.00$

Even the scale interaction matrices are only able to show accurately the average contribution of one scale to another, namely the sum over all wavelets of a given scale.

The few tools we built and used for this brief analysis show how it is possible to use wavelets to measure energy transfers between scales in a sampled solution to a model equation. Even our very simple examples contain some obstacles to a straightforward analysis, such as shift artifacts. Nevertheless these first results could be considered rather encouraging. Moreover, considering our very preliminary results, the same wavelet description of the propagation phenomenon seems to be useful even in the two dimensional case.

7 Acknowledgments

All computations were performed on an unloaded NeXT workstation, using a combination of *Mathematica* [14] and the *Adapted Waveform Analysis* library of C functions [8].

List of Figures

References

[1] G. K. Batchelor. The theory of axisymmetric turbulence. *Proceedings of the Royal Society (London)*, A106(1007):480–502, 1946.

[2] R. Benzi, M. Briscolini, M. Colella, and P. Santangelo. A simple point vortex model for two-dimensional decaying turbulence. *Physics of Fluids*, 15:1036–1039, 1992.

[3] R. Benzi and B. Legras. Wave-vortex dynamics. *Journal of Physics A: Mathematics and General Physics*, 20:5125–5144, 1987.

[4] Gregory Beylkin, Ronald R. Coifman, and Vladimir Rokhlin. Fast wavelet transforms and numerical algorithms I. *Communications on Pure and Applied Math*, XLIV:141–183, 1991.

[5] J. M. Burgers. . *Proceedings of the Royal Academy of Sciences, Amsterdam*, 26:582, 1923.

[6] Ingrid Daubechies. Orthonormal bases of compactly supported wavelets. *Communications on Pure and Applied Mathematics*, XLI:909–996, 1988.

[7] Marie Farge, Eric Goirand, Yves Meyer, Frédéric Pascal, and Mladen Victor Wickerhauser. Improved predictability of two-dimensional turbulent flows using wavelet packet compression. *Fluid Dynamics Research*, 10:229–250, 1992.

[8] Fast Mathematical Algorithms and Hardware Corporation, Hamden, Connecticut. *Adapted Waveform Analysis Library, v2.0*, June 1992. Software Documentation.

[9] Washington University in St. Louis. wuarchive. InterNet Anonymous File Transfer (ftp) Site wuarchive.wustl.edu [128.252.135.4], 1991–present.

[10] A. N. Kolmogorov. The local structure of turbulence in incompressible viscous fluids for very large Reynolds numbers. *Doklady Akademii Nauk SSSR*, 30:301–305, 1941. In Russian.

[11] Robert H. Kraichnan. Statistical dynamics of two-dimensional flow. *Journal of Fluid Mechanics*, 67, part 1:155–175, 1975.

[12] J. Liandrat and Philippe Tchamitchian. Resolution of the 1-D regularized Burgers equation using a spatial wavelet approximation — algorithm and numerical results. *ICASE report*, 1990. Was also published with Valerie Perrier in a shorter form in [13].

[13] Mary Beth Ruskai et al., editors. *Wavelets and Their Applications*. Jones and Bartlett, Boston, 1992. ISBN 0-86720-225-4.

[14] Steven Wolfram, Thomas W. Gray, and Douglas Stein. Mathematica: a system for doing mathematics by computer. Available from Wolfram Research Incorporated, P.O. Box 6059, Champaign, IL 61821, 1992. Version 2.0 for NeXT computers.

[15] N. J. Zabusky. Contour dynamics: a method for inviscid and nearly inviscid two-dimensional flows. In T. Tatsumi, editor, *Proceedings of the IUTAM Symposium on Turbulence and Chaotic Phenomena*, pages 251–257. North-Holland, 1984.